



ELSEVIER

journal homepage: www.intl.elsevierhealth.com/journals/cmpb

Analysis of three T1DM simulation models for evaluating robust closed-loop controllers

P. Colmegna¹, R.S. Sánchez Peña*,²

Centro de Sistemas y Control, Departamento de Matemática, Instituto Tecnológico de Buenos Aires (ITBA), Av. Eduardo Madero 399, C1106ACD Buenos Aires, Argentina

ARTICLE INFO

Article history:

Received 16 October 2012

Received in revised form

19 September 2013

Accepted 25 September 2013

Keywords:

Diabetes mellitus simulators

Diabetes control

Robust control

ABSTRACT

This work compares three well-known models and simulators in terms of their use in the analysis and design of glucose controllers for patients with Type 1 Diabetes Mellitus (T1DM). The objective is to compare them in practical scenarios which include: model uncertainty, time variance, nonlinearities, glucose measurement noise, delays between subcutaneous and plasma levels, pump saturation, and real-time controller implementation. The pros and cons of all models/simulators are presented. Finally, the simulators are tested with different robust controllers in order to identify the difficulties in the design and implementation phases. To this end, three sources of uncertainty are considered: nonlinearities, time-varying behavior (intra-patient) and inter-patient differences.

© 2013 Elsevier Ireland Ltd. All rights reserved.

1. Introduction

The artificial automatic control of glucose for patients with Type 1 Diabetes Mellitus has been a long-standing objective since the creation of continuous glucose monitors and insulin pumps [1]. The Artificial Pancreas Project launched by the Juvenile Diabetes Research Foundation (JDRF) in 2005 generated a great deal of research in this area in the last few years.

In order to design an automatic controller that may connect a glucose monitor and an insulin pump, a model of the underlying dynamics is generally necessary. To verify the effectiveness of the controller before clinical tests, several *in silico* evaluations should be performed. To this end, a more elaborate dynamic model which includes not only the glucose-insulin behavior, but also many other practical issues (insulin pump constraints, glucose monitor errors, interstitial-plasma delays) should be implemented as a simulator.

A few models based upon ordinary differential equations (ODE) have been used for simulation and control design purposes [2,3,1,4]. Among the initial ones we can mention Sorensen's 19th order model [5] and Bergman's 3rd. order model [6]. One of the first control algorithms was presented in 1991 by Fisher [7] and was based on [6], and more sophisticated models and controllers have been developed since then. Many of them are instrumental for patient analysis, like the AIDA freeware available at <http://www.2aida.org/aida/intro.htm> [8], while others are also used for automatic controller design and testing. The aim of this work is to present a comparison between the most relevant models in this last group, which can be considered to be the standards in terms of controller performance analysis.

Controller design for this process has been approached in different ways using different models (see [1] for a survey). Solutions go from simple PID control to heuristic fuzzy-logic procedures or parametric-programming [9]. The

* Corresponding author. Tel.: +54 1163934853.

E-mail addresses: pcolme@al.u.itba.edu.ar (P. Colmegna), rsanchez@itba.edu.ar (R.S. Sánchez Peña).

¹ PhD student at ITBA and Lecturer at Universidad Nacional de Quilmes.

² PhD Program Director at ITBA and Investigador Principal, CONICET.

0169-2607/\$ – see front matter © 2013 Elsevier Ireland Ltd. All rights reserved.

<http://dx.doi.org/10.1016/j.cmpb.2013.09.020>

aforementioned models present significant sources of uncertainty that are worth considering. Robust Control Theory [10–12] has been applied to this problem, centered on the uncertainty issue. Also, a Linear Parameter Varying (LPV) model has been derived in [13] based on Sorensen's model and controlled by an H_∞ linear time invariant (LTI) control in [14,15]. In addition, due to the nature of the dynamics in all models, MPC [16–18], nonlinear control design methods [19,20], LPV and Unfalsified control (UC) [21,22], have also been applied. Based on the latter, attention should be paid to all of the following issues:

- Model uncertainty (dynamics, intra- and inter-patient).
- Nonlinear phenomena.
- Time delays, actuator saturation, measurement noise.
- Real-time implementation.

The objective of this work is to compare the three main models which are used in controller (closed-loop) testing: Sorensen's 19th order model [5], the model developed by the Universities of Virginia and Padova (UVa/Padova) [23] and the Cambridge model [18]. The two latter ones have been implemented in the form of simulators as well. As a byproduct of our research, several errors in the literature have been found and are pointed out in order to help the practitioner when programming these models [12].

Another important point is their use in controller synthesis and implementation in practical situations which should include all the issues mentioned previously. In particular, robust controllers should cope with model uncertainty. Hence, three sources of uncertainty (nonlinearities, inter- and intra-patient variations) are considered. The first is interpreted as model variations among different linearization points. The last one considers the time-varying behavior within a certain patient. The time delays, actuator saturation and measurement noise will be included in the design as part of the synthesis weights and also in the closed-loop simulation tests.

The paper is organized as follows. Sections 2–4 describe the three aforementioned dynamic models and simulators, respectively. Section 5 compares them from different points of view. Section 6 is devoted to the application of these models/simulators to controller design and to performance results obtained from these robust controllers. Final conclusions are drawn in Section 7.

2. Sorensen's model

Sorensen's mathematical model is an explanatory physiological mechanism of the glucose metabolism in a normal average man. It divides the body into six compartments: (1) brain, representing the central nervous system; (2) heart and lungs; (3) gut; (4) liver; (5) kidneys and (6) muscular skeleton and adipose tissue (peripheral). In addition, each compartment is composed of three spaces: (1) blood capillary, fed by the arterial blood and evacuated by the venous one; (2) interstitial and (3) intracellular. Nevertheless, the number of spaces can be reduced to two or to one, depending

on the permeability of the membranes in each compartment.

In Sorensen's formulation three models interact: glucose, insulin and glucagon. In order to obtain a mathematical representation, a mass balance is performed in each physiological compartment. As a consequence, 12 nonlinear ordinary differential equations are obtained for the glucose (three associated to non dimensional variables) and glucagon dynamics and seven linear ones for the insulin. It is important to note that the linearity in the insulin model is due to the fact that diabetes type I is considered. This assumption not only induces linearity, but also decouples the insulin dynamics from the others. The glucose absorption model in [8] is used by several other authors [11,13–15], as well as in the AIDA simulator, instead of the original one employed in [5]. A close analysis of the dynamic equations (see [Appendix A](#)) indicates several inconsistencies with respect to the models presented in previous works (see also [12]). For example in [13], variable A_{IHGU} is confused with A_{IHGP} in Eq. (4). In the same work, there are no parenthesis in Eq. (3) and there are numerical differences in Eq. (7). Also in Eq. (5) the denominator should read T_p^l/V_p^T instead of $1/T_p^l V_p^T$. These last three errors are also present in [11]. In Eq. (2) of [10], instead of V_p^C we find V_p^T , which does not allow its simplification. All these can always be interpreted as typing errors. Nevertheless, there is a common error in all of these works and also in [1] which concerns Eq. (6). The variable which should be there is not I_K^C , but I_H^C instead. This error already appears in the original work [5] in the section where the complete model is presented (pages 213–222), but the correct variable can be identified through the analysis of page 134 over Γ_{KC} , where the article [24] is referenced. The latter can be also ratified by the programming instructions of the model in [5] on page 535.

3. UVa/Padova's model/simulator

This model is presented in [25] and divides the body into two subsystems: glucose and insulin, each divided into two compartments. The parameter adjustment is based on experiments over 204 normal subjects in order to obtain a non-diabetic model (a type 2 diabetic model is also obtained with another database). The GIM simulator [26] adapts the previous non-diabetic model in order to simulate a type 1 diabetic subject which includes a model of subcutaneous (s.c.) insulin kinetics. The glucose absorption model used in [25,26,23] is the one described in [27]. The complete model equations used in GIM are presented in [Appendix B](#).

The UVa/Padova Type 1 Diabetes Mellitus Simulator (T1DMS), which is based on the previous model, is presented in [23]. Its distributed version can be obtained through the UVa/Padova organization, enhanced by models of insulin pumps and glucose monitors, both considered subcutaneous. The aforementioned distributed version has a cohort of 30 virtual³ patients (10 adults, 10 adolescents, 10 children). A more elaborate model with a cohort of 300 patients and

³ By virtual we mean a synthetic patient which has been designed by combining different parameters in the simulator.

Table 1 – Pros and cons of the three models/simulators.

Model/simulator	Pros	Cons
Sorensen	<ul style="list-style-type: none"> • Immediate transformation of a normal to a controlled T1DM patient • Considers glucagon dynamics 	<ul style="list-style-type: none"> • Insulin injection is intravenous
Uva/Padova	<ul style="list-style-type: none"> • Includes inter-subject variability • Has a large cohort of virtual subjects • An average T2DM patient has also been obtained through this model • A reliable glucose absorption model • Adds models of CGM and s.c. insulin delivery (specific brands) • Accepted by the FDA 	<ul style="list-style-type: none"> • Inter and intra-subject variability are not taken into account • Glucagon dynamics are not considered • Intra-subject variability is not included
Cambridge	<ul style="list-style-type: none"> • Has a cohort of in silico patients validated with a clinical study • Includes intra-subject variability • A physical exercise model is included • Adds general models of CGM and s.c. insulin delivery 	<ul style="list-style-type: none"> • Glucagon dynamics are not considered • Its glucose absorption model is oversimplified

approved by the Food and Drug Administration (FDA) to skip animal tests is not available for comparison in this work because it is not freely distributed outside the UVa/Padova organization.

4. Cambridge's model/simulator

This model has been developed by the group directed by Prof. Hovorka in Cambridge, see [28,20,18] (see Appendix C for model equations). It has 5 submodels that describe the glucose regulation in T1DM.

The dynamics presented in [18] are used in a simulator developed at the University of Cambridge. However, Eqs. (8)–(10) are inconsistent in [18]. The deactivation rate constants k_{ai} which multiply the states $x_i(t)$ should be replaced with the corresponding activation rate constants k_{bi} in all those equations, $i=1, 2, 3$. Also in that work, Eq. (11) appears with a plus sign instead of a minus sign when compared to the same equation in the simulator description document. In addition to the aforementioned submodels, Cambridge's simulator includes a submodel of physical exercise by a single parameter from a log-normal distribution representing a drop in plasma concentration. The simulator environment, which was validated against an overnight clinical study, has a virtual population of 18 subjects with T1DM and considers the s.c. glucose measurement and insulin pump delivery errors. The educational version of this simulator has only 6 virtual subjects. A subset of the individual parameters has been estimated from experimental data collected in subjects with T1DM, and others have been drawn from informed probability distributions. An important issue concerns the concept of synthetic subject. It represents the inter-subject variability when a unique set of parameters is assigned to each individual, and the intra-subject variability when certain parameters are considered to be time-varying.

In [18] the virtual subjects with T1DM were validated with clinical studies. These were carried out with an identical closed-loop control algorithm (MPC), and similar results were obtained.

5. Model/simulator comparisons

Here, some pros and cons from the different models/simulators are presented in terms of their uncontrolled (open-loop) behavior and are summarized in Table 1. The next section is devoted to comparing these simulators when applied to controller design and test.

Sorensen's model was the first complete compartmental dynamics which presented the notion of an average patient that could be tuned parametrically. It allows an immediate transformation from a normal to a controlled T1DM patient by eliminating the Γ_{PIR} factor associated to the insulin released from the pancreas. Nevertheless, it has several drawbacks. It contemplates only intravenous insulin, eliminating the significant delay in the injection of this hormone, which is of great importance from an s.c. control standpoint. Although in [5] the model capacity for predicting diabetic metabolic abnormalities is proved, it is also acknowledged that an individualized parameter adjustment is desirable. An attempt to compensate for the lack of inter-subject variability is made in [11], through the variation of some physiological parameters. Nevertheless, these parameter variations were synthesized through the T1DM model, in the absence of data from real T1DM patients.

The UVa/Padova model is also compartmental and represents an average patient that may be tuned parametrically. Still, in contrast with Sorensen's model, this one solves the inter-subject variability problem through a large cohort of virtual subjects. It includes a glucose absorption model which has several advantages with respect to the one presented in [8] (see [27]). It also adds models of continuous glucose monitoring (CGM) and s.c. insulin delivery, which allow more realistic simulations. Furthermore, this system has been accepted by the FDA as a substitute to animal trials in the pre-clinical testing of closed-loop control strategies. The drawback with respect to Sorensen's model is that here, the glucagon has not been considered.

From Cambridge's model, the following may be concluded. It is a simulation environment designed specifically to

support the development of closed-loop insulin delivery systems in T1DM, whereas in [25] an average T2DM is also obtained. The software allows for a comprehensive assessment of an individual, as well as the population *in silico* study results. The validity of population-based predictions generated by this simulation environment was demonstrated by comparison with a clinical study in young subjects with T1DM in an overnight evaluation (see [18]). This is an advantage with respect to the UVa/Padova simulation environment which was not validated by clinical trials, but by synthetic ones instead. Two other advantages are: the intra-subject variability is induced by adopting time-varying parameters, and a physical exercise model is included. The drawback is that, similarly to the UVa/Padova model, the glucagon has not been considered. Finally, the hormonal effects of epinephrine, growth hormone and cortisol have been neglected in all these models.

6. Application to controller synthesis and testing

6.1. Sorensen's model

Since there is no simulator for Sorensen's model, a Simulink model was developed, which also includes random and filtered noise for the glucose measurement with an inaccuracy of 5%⁴ and an insulin pump saturation of 100 mU/min (see [9]). The insulin injection here is intravenous.

The nonlinear model is linearized at nine different interstitial glucose concentrations which range from 2.56 to 10.17 mmol/ℓ. The low level of nonlinearity allows the representation of the system as a nominal LTI model plus uncertainty. The nominal model can be reduced from 19 to 6 states with no major impact. A discrete H_∞ controller is designed based on a mixed-sensitivity performance objective defined as:

$$\min \left\{ \gamma \text{ such that } \left\| \begin{bmatrix} W_p(z)S(z) \\ W_\Delta(z)K(z)S(z) \end{bmatrix} \right\|_\infty < \gamma \right\}$$

where $S(z) = (I + GK)^{-1}$ is the sensitivity function, $W_p(z)$ and $W_\Delta(z)$ are the performance and additive uncertainty weights, respectively, and $K(z)$ is the controller.

The design is performed via the H_∞ optimal control method using the loop-shifting formulae of [30], considering the following weights:

$$W_p(z) = \frac{0.015z + 0.015}{z - 0.999990}$$

$$W_\Delta(z)$$

$$= \frac{0.0002494z^3 + 0.0001069z^2 + 8.882 \times 10^{-16}z - 2.22 \times 10^{-16}}{z^3 - 2.797z^2 + 2.606z - 0.8084}$$

The controller, which provides stability and performance at all different working points, operates with a sampling time of

⁴ The American Diabetes Association (ADA) has suggested that meter systems should have an inaccuracy of less than 5% [29]. Nevertheless, current continuous glucose monitors have not yet achieved that accuracy.

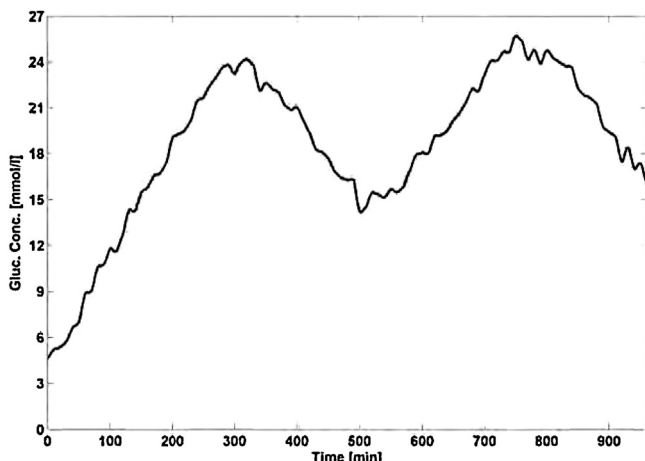


Fig. 1 – Uncontrolled simulation in Sorensen's model.

1 min and has order 10 with a $\gamma = 0.9683$. In this simulation, the evolution of an average normal patient perturbed as in [10] was used as a reference, starting from an initial concentration value of 4.85 mmol/ℓ. The results of two glucose intakes of 100 g each are depicted in Figs. 1 and 2. Fig. 1 is associated with the uncontrolled scenario without insulin infusion (open-loop) and Fig. 2, with the average type 1 diabetic patient with the controller in place (closed-loop).

6.2. UVa/Padova's simulator

The database of T1DMS and GIM were used to obtain a discrete H_∞ robust controller which could handle three different patients with T1DM. One of the patients was the average one proposed in [26]. These three models were linearized around the glucose level of 5.1 mmol/ℓ. The same design technique used in Sorensen's model was used here, but considering the following weights:

$$W_p(z) = \frac{0.001075z + 0.001075}{z - 0.999970}$$

$$W_\Delta(z) = \frac{0.000127z^2 + 0.000244z + 0.0001172}{z^2 - 1.993z + 0.993}$$

Also, the same sampling time and measurement noise as in Sorensen's model were used,⁵ and an insulin pump saturation of 30 U/h (OmniPod) was included. The designed controller has order 16 and is reduced to order 6 with a $\gamma = 2.5359$.

In Fig. 3, the open-loop simulation of all three patients is depicted, and in Fig. 4, their controlled responses with two glucose perturbations of 100 g each one are represented. In the controlled simulations, the evolution of the average normal patient was used as a reference, according to the parameters presented in [25].

⁵ The authors wanted to compare the controlled simulations with similar measurement error characteristics.

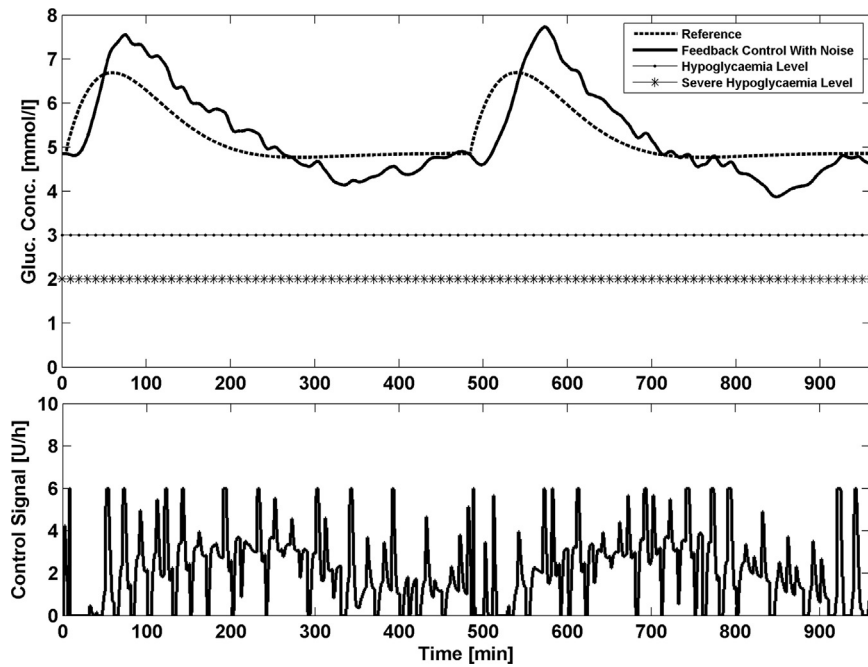


Fig. 2 – Closed-loop simulation of Sorensen's model with the discrete H_∞ controller.

6.3. Cambridge's simulator

As mentioned previously, the advantage of this simulator is the intra-patient variability representation when considering time-varying parameters. Hence, the strategy here is a linearization of the nonlinear dynamics at different sampling times but with a constant interstitial glucose concentration. The first virtual subject (there are six in the Simulator Educational Version) at {0, 60, 120} min and a concentration of 5.10 mmol/ℓ was considered. The parameter variation in this simulator is periodic, hence parameters at 0 and 180 min are repeated.

Based on these 3 models and after repeating the procedure followed in the previous designs, a discrete H_∞ controller is

obtained which guarantees stability and performance. In this case, the design is achieved using LMI optimization ([31]) and considers the following weights:

$$W_p(z) = \frac{0.00475z + 0.00475}{z - 0.999990}$$

$$W_d(z) = \frac{3.177 \times 10^{-6}z^2 + 6.354 \times 10^{-6}z + 3.177 \times 10^{-6}}{z^2 - 1.994z + 0.9935}$$

A controller of order 11 is obtained and is reduced to order 9 with a $\gamma = 1$. As a consequence it allows, after an ingestion, the average plasma glucose level to return to a constant and safe value. In Fig. 5, the simulated uncontrolled response of the patient after two glucose intakes of 100 g each is represented. Figs. 6 and 7 plot the controlled (closed-loop) response of the same patient with the MPC controller proposed in the simulator and the H_∞ controller, respectively.

All simulations are based on the following conditions:

- No bolus is applied previous to food ingestion.
- The sampling time and controller application interval is 1 min.
- Glucose measurements and insulin injection are both subcutaneous.
- The variation coefficient (CV) of the error in the continuous insulin injection for the calibration and for the glucose measurement errors are all 5%.

The closed-loop simulations show that the MPC signal is not enough to guarantee a good performance by itself. For this reason, a pre-meal insulin bolus is used in these cases. The aim of this research is to obtain a control signal without any correction bolus, hence the H_∞ controller seems to be better than MPC in this case.

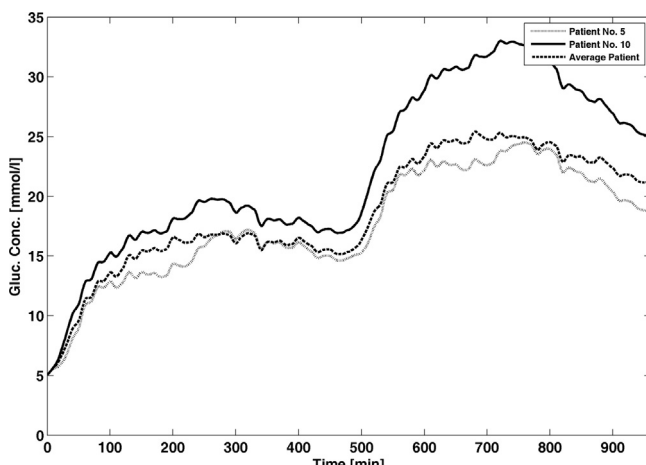


Fig. 3 – Uncontrolled simulation for Nos. 5, 10 and average patients of UVa/Padova's simulator.

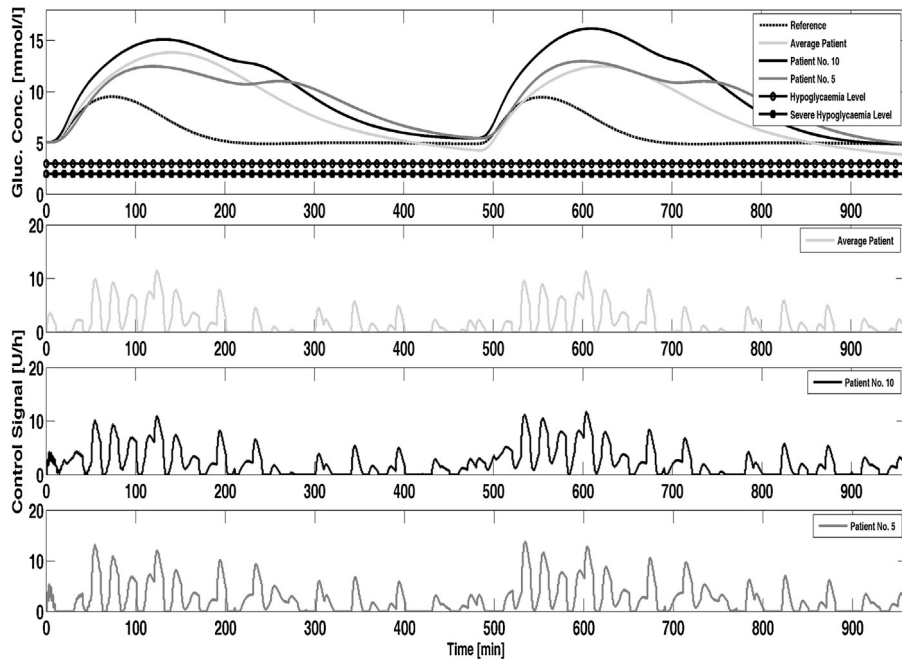


Fig. 4 – Closed-loop simulation for Nos. 5, 10 and average patients of UVa/Padova's simulator with the discrete H_∞ controller.

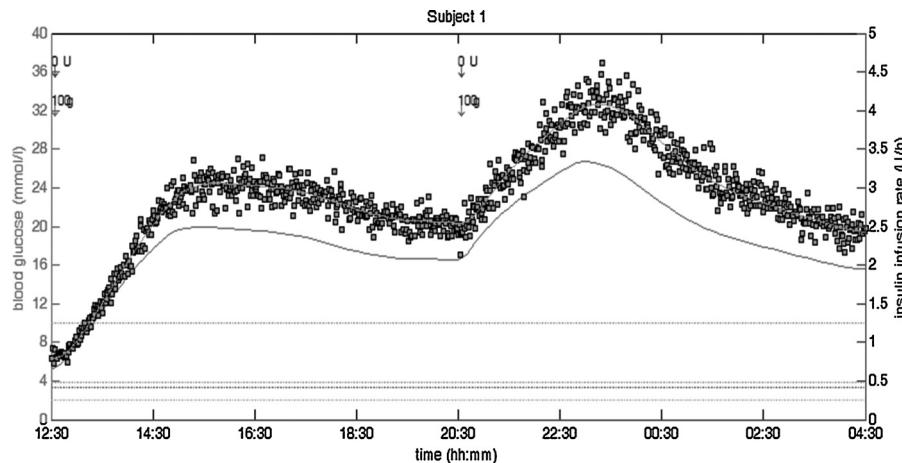


Fig. 5 – Open-loop simulation of Cambridge's model. The continuous lines are the plasma glucose concentration and the insulin injection rate, the squares are glucose measurements, and the dash lines are the desired glucose range (3.9 to 8 mmol/l), the hypoglycaemia level (3 mmol/l), and the severe hypoglycaemia level (2 mmol/l).

7. Conclusions and future research

Comparisons are always difficult and no single answer is possible. Besides the differences between the simulation environments pointed out in Section 5, the possibility of design and simulation of controlled patients is also fundamental, as illustrated in Section 6. The 4 items mentioned in Section 1 need to be achieved, and in that sense, the inter- and intra-patient variability cannot be represented adequately in all of these models, except for Cambridge's model. On the other hand the FDA approval, which skips animal testing, is only

possible for the complete UVa/Padova's simulator, although through a synthetic validation method. Finally, Sorensen's model has as a unique advantage over the other two ones: the inclusion of glucagon, which could be relevant in future control approaches. From the computational point of view, the Cambridge simulator is slower due to the fact that many text files are generated in the process.

In this work, the design and simulation of closed-loop controlled patients have been instrumental as an application of the previous model/simulator analysis. As for (robust) control issues, here the uncertainty has been represented by nonlinearities, inter- and intra-patient variations, the latter as a

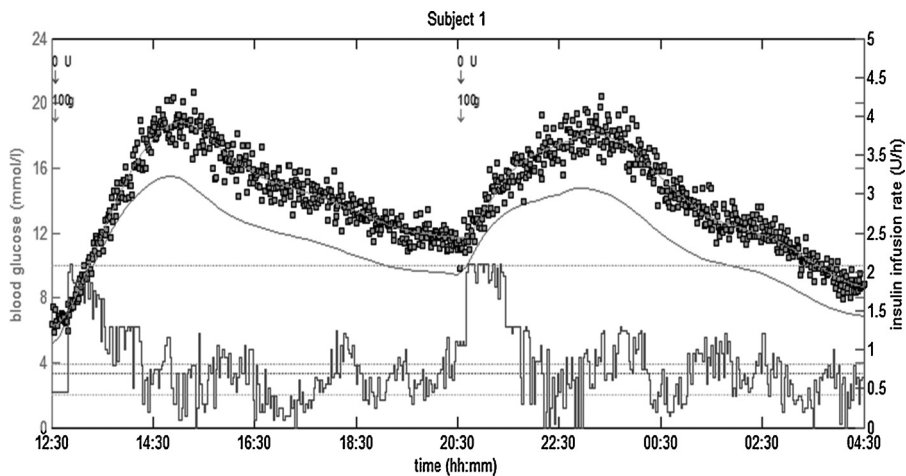


Fig. 6 – Simulation of Cambridge's model with their proposed MPC. The line indications are the same as the ones in Fig. 5.

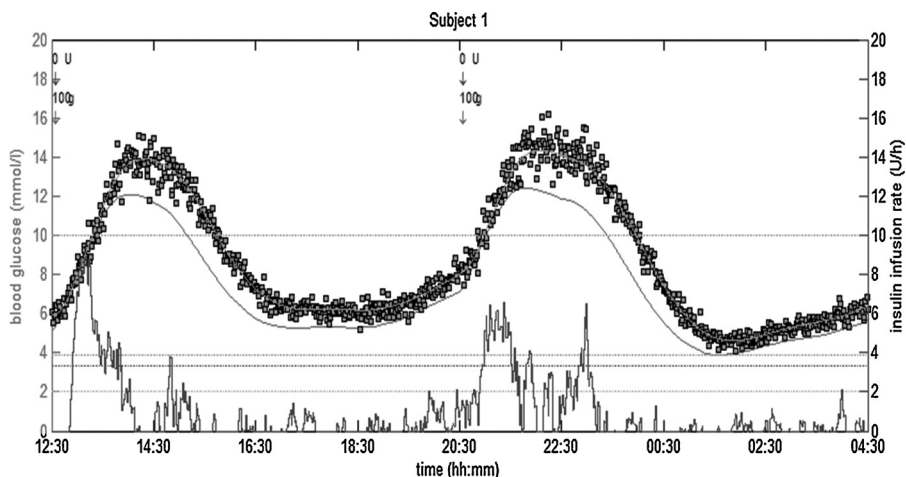


Fig. 7 – Simulation of Cambridge's model with the discrete H_∞ control. The line indications are the same as the ones in Fig. 5.

time-varying behavior. For these three sources of uncertainty and with different discrete H_∞ robust controllers applied to three different simulations, a satisfactory answer has been achieved. Nevertheless, the most accurate control seems to be achieved by Sorensen's model. This is because the interstitial-plasma delay in the control signal and the inter- and intra-subject variability are not included. Therefore, and as Figs. 4 and 7 indicate, more realistic scenarios induce a more difficult problem, and hence less performance. Also, it tends to be harder when a single controller is used to control a group of T1DM patients. In a real situation, all three sources of uncertainty mentioned above should be considered simultaneously. In that case, most probably a robust LTI controller such as the one designed here would not be enough. Therefore, a thorough exploration of nonlinear and/or linear time-varying (LTV) controllers should be attempted. Some previous results have been achieved with MPC [16–18], and by the authors with LPV and UC as well [21,22], but further research is needed before a reliable closed-loop behavior without *a priori* calibration, and

useful for a large variety of patients, can be obtained in clinical tests.

Conflict of interest statement

The authors have no financial or personal conflict of interest.

Acknowledgments

Both authors were supported by the program PRH No. 71 (PICT 290 and PFDT) of the Ministry of Science, Technology and Innovation of Argentina. We wish to thank Dr. Jorge Bondía for his helpful comments and suggestions. We are also grateful to Prof. Hovorka's group in Cambridge for allowing us to use their simulator. Finally, we also wish to thank Dr. Gosia Wilinska, who answered all our questions so patiently.

Appendix A. Sorensen's model equations ([5,15])

- Glucose dynamics:

$$\begin{aligned}
 \dot{G}_B^C &= (G_B^C - G_B^T) \frac{q_B}{V_B^C} - (G_B^C - G_B^T) \frac{V_B^T}{T_B V_B^C} \\
 \dot{G}_B^T &= (G_B^C - G_B^T) \frac{1}{T_B} - \frac{\Gamma_{BU}}{V_B^T} \\
 \dot{G}_H^C &= (G_B^C q_B + G_L^C q_L + G_K^C q_K + G_P^C q_P - G_H^C q_H - \Gamma_{RBCU}) \frac{1}{V_H^C} \\
 \dot{G}_S^C &= (G_H^C - G_S^C) \frac{q_S}{V_S^C} + \frac{\Gamma_{meal}}{V_S^C} - \frac{\Gamma_{SU}}{V_S^C} \\
 \dot{G}_L^C &= (G_H^C q_A + G_S^C q_S - G_L^C q_L) \frac{1}{V_L^C} + \frac{\Gamma_{HGP}}{V_L^C} - \frac{\Gamma_{HGU}}{V_L^C} \\
 \dot{G}_K^C &= (G_H^C - G_K^C) \frac{q_K}{V_K^C} - \frac{\Gamma_{KE}}{V_K^C} \\
 \dot{G}_P^C &= (G_H^C - G_P^C) \frac{q_P}{V_P^C} + (G_P^T - G_P^C) \frac{V_P^T}{T_P^G V_P^C} \\
 \dot{G}_P^T &= (G_P^C - G_P^T) \frac{1}{T_P^G} - \frac{\Gamma_{PGU}}{V_P^T}
 \end{aligned} \tag{1}$$

- Insulin dynamics:

$$\begin{aligned}
 i_B^C &= (I_H^C - I_B^C) \frac{Q_B}{V_B^C} \\
 i_H^C &= (I_B^C Q_B + I_L^C Q_L + I_K^C Q_K + I_P^C Q_P - I_H^C Q_H + \Gamma_{IVI}) \frac{1}{V_H^C} \\
 i_S^C &= (I_H^C - I_S^C) \frac{Q_S}{V_S^C} \\
 I_L^C &= (I_H^C Q_A + I_S^C Q_S - I_L^C Q_L) \frac{1}{V_L^C} + \frac{\Gamma_{PIR}}{V_L^C} - \frac{\Gamma_{LC}}{V_L^C} \\
 i_K^C &= (I_H^C - I_K^C) \frac{Q_K}{V_K^C} - \frac{\Gamma_{KC}}{V_K^C} \\
 i_P^C &= (I_H^C - I_P^C) \frac{Q_P}{V_P^C} + (I_P^T - I_P^C) \frac{V_P^T}{T_P^I V_P^C} \\
 i_P^T &= (I_P^C - I_P^T) \frac{1}{T_P^I} + \frac{\Gamma_{SIA}}{V_P^T} - \frac{\Gamma_{PC}}{V_P^T}
 \end{aligned} \tag{2}$$

- The remaining 4 equations:

$$\begin{aligned}
 \dot{N} &= (\Gamma_{PNR} - N) \frac{F_{PNC}}{V_N} \\
 \dot{A}_{IHGP} &= \frac{1}{25} \left\{ 1.2088 - 1.138 \tanh \left[1.1669 \left(\frac{I_L^C}{21.43} - 0.8885 \right) \right] - A_{IHGP} \right\} \\
 \dot{A}_{NHGP} &= \frac{1}{65} \left[\frac{2.7 \tanh(0.388N) - 1}{2} - A_{NHGP} \right] \\
 \dot{A}_{IHGU} &= \frac{1}{25} \left[2 \tanh \left(0.549 \frac{I_L^C}{21.43} \right) - A_{IHGU} \right]
 \end{aligned} \tag{3}$$

The Γ_i parameters which appear in the equations are as follows: $\Gamma_{BU} = 70$, $\Gamma_{RBCU} = 10$, $\Gamma_{SU} = 20$, $\Gamma_{PIR} = 0$, $\Gamma_{LC} = F_{LC}(I_H^C Q_A + I_S^C Q_S + \Gamma_{PIR})$ and

$$\begin{aligned}
 \Gamma_{HGU} &= 20A_{IHGU} \left\{ 5.6648 + 5.6589 \tanh \left[2.4375 \left(\frac{G_L^C}{101} - 1.48 \right) \right] \right\} \\
 \Gamma_{HGP} &= 155A_{IHGP}[2.7 \tanh(0.388N) - A_{NHGP}] \times \left\{ 1.425 - 1.406 \tanh \left[0.1699 \left(\frac{G_L^C}{101} - 0.4969 \right) \right] \right\}
 \end{aligned} \tag{4}$$

$$\begin{aligned}\Gamma_{PGU} &= \frac{35G_P^T}{86.81} \left\{ 7.035 + 6.51623 \tanh \left[0.33827 \left(\frac{I_P^T}{5.304} - 5.82113 \right) \right] \right\} \\ \Gamma_{PNR} &= \left\{ 1.3102 - 0.61016 \tanh \left[1.0571 \left(\frac{I_H^C}{15.15} - 0.46981 \right) \right] \right\} \times \left\{ 2.9285 - 2.095 \tanh \left[4.18 \left(\frac{G_H^C}{91.89} - 0.6191 \right) \right] \right\} \\ \Gamma_{PC} &= \frac{I_P^T}{(1 - F_{PC})/(Q_P F_{PC}) - T_P^I/V_P^T}\end{aligned}\quad (5)$$

$$\Gamma_{KC} = F_{KC} I_H^C Q_K \quad (6)$$

$$\Gamma_{KE} = \begin{cases} 71\{1 + \tanh[0.11(G_K^C - 460)]\} & \text{if } G_K^C < 460 \text{ mg/dl} \\ 0.872G_K^C - 330 & \text{if } G_K^C \geq 460 \text{ mg/dl} \end{cases} \quad (7)$$

Notation

Indices

A: Hepatic artery	B: Brain	BU: Brain uptake
C: Capillary space	G: Glucose	H: Heart and lungs
HGP: Hepatic glucose production.	HGU: Hepatic glucose uptake	I: Insulin
IHGP: Insulin effect on HGP	IHGU: Insulin effect on HGU	IVI: Intravenous insulin infusion
K: Kidney	KC: Kidney clearance	KE: Kidney excretion
L: Liver	LC: Liver clearance	N: Glucagon
NHGP: Glucagon effect on HGP	P: Periphery (muscle/adipose tissue)	PC: Peripheral clearance
PC: Peripheral clearance	PGU: Peripheral glucose uptake	PIR: Pancreatic insulin release
PNC: Pancreatic glucagon clearance	PNR: Pancreatic glucagon release	RBCU: Red blood cell uptake
S: Gut	SIA: Insulin absorption into blood stream from subcutaneous depot	SU: Gut uptake
T: Tissue		

Variables

A: Auxiliary equation state	F: Fractional clearance	G: Glucose concentration
I: Insulin concentration	N: Glucagon concentration (normalized)	Q: Vascular plasma flow rate
q: Vascular blood flow rate	T: Transcapillary diffusion time constante	V: Volume (L)
v: Volume (dL)	I: Metabolic source or sink rate	

Appendix B. UVa/Padova model equations ([25,26])

- Glucose subsystem:

$$\begin{aligned}\dot{G}_p(t) &= EGP(t) + Ra(t) - U_{ii}(t) - E(t) - k_1 G_p(t) + k_2 G_t(t) \\ \dot{G}_t(t) &= -U_{id}(t) + k_1 G_p(t) - k_2 G_t(t) \\ G(t) &= \frac{G_p(t)}{V_G} \\ EGP(t) &= k_{p1} - k_{p2} G_p(t) - k_{p3} I_d(t) \\ fQ_{sto} &= Q_{sto1}(t) + Q_{sto2}(t) \\ \dot{Q}_{sto1}(t) &= -k_{gri} Q_{sto1}(t) + D\delta(t) \\ \dot{Q}_{sto2}(t) &= -k_{empt} (Q_{sto}) Q_{sto2}(t) + k_{gri} Q_{sto1}(t) \\ \dot{Q}_{gut}(t) &= -k_{abs} Q_{gut}(t) + k_{empt} (Q_{sto}) Q_{sto2}(t) \\ Ra(t) &= \frac{f k_{abs} Q_{gut}}{BW} \\ U_{ii}(t) &= F_{cns} \\ U_{id}(t) &= \frac{V_m(X) G_t(t)}{K_{m0} + G_t(t)} \\ V_m(X) &= V_{m0} + V_{mx} X(t) \\ \dot{X}(t) &= -p_{2U} X(t) + p_{2U} [I(t) - I_b] \\ E(t) &= \begin{cases} k_{e1}[G_p(t) - k_{e2}], & G_p(t) > k_{e2} \\ 0, & G_p(t) \leq k_{e2} \end{cases}\end{aligned}$$

- Insulin subsystem:

$$\begin{aligned}\dot{I}_\ell(t) &= -[m_1 + m_3] I_\ell(t) + m_2 I_p(t) \\ \dot{I}_p(t) &= -(m_2 + m_4) I_p(t) + m_1 I_\ell(t) + k_{a1} I_{sc1}(t) + k_{a2} I_{sc2}(t) \\ I(t) &= \frac{I_p(t)}{V_I} \\ \dot{I}_1(t) &= -k_i (I_1 - I)(t) \\ \dot{I}_d(t) &= -k_i (I_d - I_1)(t) \\ \dot{I}_{sc1} &= -(k_d + k_{a1}) I_{sc1}(t) + IIR(t) \\ \dot{I}_{sc2} &= k_d I_{sc1}(t) - k_{a2} I_{sc2}(t)\end{aligned}$$

Notation

G_p : Glucose mass in plasma and rapidly equilibrating tissues	G_t : Glucose mass in slowly equilibrating tissues	G : Plasma glucose concentration
EGP: Endogenous glucose production	R_a : Glucose rate of appearance in plasma	E : Renal excretion
U_{ii} and U_{id} : Insulin-independent and -dependent glucose utilizations	V_G : Distribution volume of glucose	k_1 and k_2 : Rate parameters
I_p and I_l : Insulin masses in plasma and in liver	I : Plasma insulin concentration	S : Insulin secretion
V_I : Distribution volume of insulin	m_1, m_2, m_3 and m_4 : Rate parameters	I_d : Delayed insulin signal
I_1 : Insulin signal associated with I_d	k_{p1} : Extrapolated EGP at zero glucose and insulin	k_{p2} : Liver glucose effectiveness
k_{p3} : Parameter governing amplitude of insulin action on the liver	k_i : Rate parameter accounting for delay between insulin signal and insulin action	Q_{sto1} and Q_{sto2} : Amount of glucose in the stomach at solid and liquid phase
Q_{gut} : Glucose mass in the intestine	k_{gri} : Rate of gridding	k_{empt} : Rate constant of gastric emptying
k_{abs} : Rate constant of intestinal absorption	f : Fraction of intestinal absorption which actually appears in plasma	D : Amount of ingested glucose
BW: Body weight	R_a : Appearance rate of glucose in plasma	F_{cns} : Glucose uptake by the brain and erythrocytes
$V_m(X)$ and K_{m0} : Parameters from the Michaelis-Menten equation	X: Insulin in the interstitial fluid	k_{e1} : Glomerular filtration rate
k_{e2} : Renal threshold of glucose	k_d : Rate constant of insulin dissociation	k_{a1} and k_{a2} : Rate constants of nonmonomeric and monomeric insulin absorption
I_{sc1} : Amount of nonmonomeric insulin in the subcutaneous space	I_{sc2} : Amount of monomeric in the subcutaneous space	IIR: Exogenous insulin infusion rate

Appendix C. Cambridge's model equations ([18])

- Insulin action submodel:

$$\dot{x}_1(t) = -k_{b1}x_1(t) + S_{IT}k_{b1}I(t) \quad (8)$$

$$\dot{x}_2(t) = -k_{b2}x_2(t) + S_{ID}k_{b2}I(t) \quad (9)$$

$$\dot{x}_3(t) = -k_{b3}x_3(t) + S_{IE}k_{b3}I(t) \quad (10)$$

- Glucose submodel:

$$\begin{aligned} \dot{Q}_1(t) &= -\left[\frac{F_{01}^c}{V_G G(t)} + x_1(t)\right] Q_1(t) + k_{12}Q_2(t) - F_R + EGP(t) + U_G(t) \\ \dot{Q}_2(t) &= x_1(t)Q_1(t) - [k_{12} + x_2(t)]Q_2(t) \\ y(t) &= G(t) = \frac{Q_1(t)}{V_G} \\ EGP(t) &= \begin{cases} EGP_0[1 - x_3(t)], & EGP \geq 0 \\ 0 & EGP < 0 \end{cases} \end{aligned} \quad (11)$$

$$\begin{aligned} F_{01}^c &= \frac{F_{01}^s G}{G + 1} \\ F_R(t) &= \begin{cases} R_{cl}(G - R_{thr})V_G, & G \geq R_{thr} \\ 0 & G < R_{thr} \end{cases} \end{aligned}$$

- Subcutaneous insulin absorption/kinetics submodel:

$$\begin{aligned} \dot{S}_1(t) &= u(t) - k_a S_1(t) \\ \dot{S}_2(t) &= k_a S_1(t) - k_a S_2(t) \\ \dot{I}(t) &= \frac{k_a S_2(t)}{V_1} - k_e I(t) \end{aligned}$$

- Gut absorption submodel:

$$\begin{aligned} \dot{G}_1(t) &= -\frac{G_1(t)}{t_{max}} + BioD(t) \\ \dot{G}_2(t) &= \frac{G_1(t)}{t_{max}} - \frac{G_2(t)}{t_{max}} \\ U_G &= \frac{G_2(t)}{t_{max}} \\ t_{max} &= \begin{cases} t_{max_ceil}, & U_G > U_{G_ceil} \\ t_{max} & U_G \leq U_{G_ceil} \end{cases} \end{aligned}$$

- Interstitial glucose submodel:

$$\dot{C}(t) = k_{a_int}(G - C)(t)$$

Here $F_{01}^s = F_{01}/0.85$, $t_{max_ceil} = G_2/U_{G_ceil}$, $S_{IT} = k_{a1}/k_{b1}$, $S_{ID} = k_{a2}/k_{b2}$, $S_{IE} = k_{a3}/k_{b3}$ and $F_{01}^s = F_{01}/0.85$.

Notation

Q_1 and Q_2 : Masses of glucose in accesible and non-accesible compartment

U_G : Gut absorption rate

G : Measured glucose concentration

I : Plasma insulin concentration

U_I : Insulin mass in plasma

k_{b1} and k_{b2} : Deactivation rate constants

R_{cl} : Renal clearance constant

k_a : Insulin absorption rate constante

$D(t)$: Amount of carbohydrates ingested

$k_{a,int}$: Transfer rate constant

k_{12} : Transfer rate constant from the non-accesible to the accesible compartment

F_{01}^c : Total non-insulin dependent glucose flux

EGP : Endogenous glucose production

x_1 , x_2 and x_3 : Remote effect of insulin on glucose distribution, disposal and EGP

k_e : Elimination rate constant for plasma insulin

k_{b3} : Deactivation rate constant for the insulin effect on endogenous glucose production

S_1 and S_2 : Insulin masses in the accesible and non-accesible compartments

G_1 and G_2 : Glucose masses in the accesible and non-accesible compartments

Bio : Carbohydrate bioavailability of the meal

V_G : Distribution volume of glucose in the accesible compartment

F_R : Renal glucose clearance

EGP_0 : Endogenous glucose production extrapolated to the zero insulin concentration

k_{a1} , k_{a2} and k_{a3} : Activation rate constants

R_{thr} : Glucose threshold

V_I : Volume of distribution of plasma insulin

u : Administration of rapid-acting insulin

t_{max} : Time-to-maximum appearance rate of glucose in the accesible compartment

C : Glucose concentration in the subcutaneous tissue

REFERENCES

- [1] F. Chee, T. Fernando, *Closed-Loop Control of Blood Glucose*, vol. 368, Springer, Berlin Heidelberg, 2007.
- [2] A. Makroglou, J. Li, Y. Kuang, Mathematical models and software tools for the glucose–insulin regulatory system and diabetes: an overview, *Applied Numerical Mathematics* 56 (2006) 559–573.
- [3] J. Bondía, J. Vehí, C. Palerm, P. Herrero, El páncreas artificial: Control automático de infusión de insulina en Diabetes Mellitus tipo I, *Revista Iberoamericana de Automática e Informática Industrial* 7 (2) (2010) 5–20.
- [4] M. Wilinska, R. Hovorka, Simulation models for *in silico* testing of closed-loop glucose controllers in type 1 diabetes, *Drug Discovery Today: Disease Models* 5 (4) (2008) 289–298.
- [5] J. Sorensen, A physiologic model of glucose metabolism in man and its use to design and assess improved insulin therapies for diabetes, Massachusetts Institute of Technology, Cambridge, MA, USA, 1985 (Ph.D. dissertation).
- [6] G. Pacini, R. Bergman, MINMOD: A computer program to calculate insulin sensitivity and pancreatic responsiveness from the frequently sampled intravenous glucose tolerance test, *Computer Methods and Programs in Biomedicine* 23 (1986) 113–122.
- [7] M. Fisher, A semiclosed-loop algorithm for the control of blood glucose levels in diabetics, *IEEE Transactions on Biomedical Engineering* 38 (1991) 57–61.
- [8] E. Lehmann, T. Deutsch, A physiological model of glucose–insulin interaction in type 1 diabetes mellitus, *Journal of Biomedical Engineering* 14 (1992) 235–242.
- [9] P. Dua, F. Doyle III, E.N. Pistikopoulos, Model-based blood glucose control for type 1 diabetes via parametric programming, *IEEE Transactions on Biomedical Engineering* 53 (8) (2006) 1478–1491.
- [10] E. Ruiz-Velázquez, R. Femat, D. Campos-Delgado, Blood glucose control for type I diabetes mellitus: a robust tracking H_∞ problem, *Control Engineering Practice* 12 (2004) 1179–1195.
- [11] R. Parker, F. Doyle III, J. Ward, N. Peppas, Robust H_∞ glucose control in diabetes using a physiological model, *AIChE Journal* 46 (12) (2000) 2537–2549.
- [12] P. Colmegna, R. Sánchez Peña, Insulin dependent diabetes mellitus control, in: Proceedings RPIC11, Oro Verde, Argentina, 2011, pp. 13–17 (selected for Special issue of Latin American Applied Research, 2012).
- [13] L. Kovács, B. Kulcsár, LPV modeling of type I diabetes mellitus, in: International Symposium of Hungarian Researchers, 2007, pp. 163–173.
- [14] L. Kovács, B. Kulcsár, J. Bokor, Z. Benyó, Model-based nonlinear optimal blood glucose control of Type I diabetes patients, in: 30th Annual International IEEE EMBS Conference, Vancouver, Canada, 2008, pp. 1607–1610.
- [15] L. Kovács, B. Benyó, J. Bokor, Z. Benyó, Induced L_2 -norm minimization of glucose–insulin system for type I diabetic patients, *Computer Methods and Programs in Biomedicine* 102 (2) (2011) 105–118.
- [16] S.D. Patek, B.W. Bequette, M. Breton, B.A. Buckingham, E. Dassau, F.J.D. III, J. Lum, L. Magni, H. Zisser, *In silico* preclinical trials: Methodology and engineering guide to closed-loop control in type 1 diabetes mellitus, *Journal of Diabetes Science and Technology* 3 (2) (2009) 269–282.
- [17] L. Magni, D.M. Raimondo, C. Dalla-Man, M. Breton, S. Patek, G.D. Nicolao, C. Cobelli, B.P. Kovatchev, Evaluating the efficacy of closed-loop glucose regulation via control-variability grid analysis, *Journal of Diabetes Science and Technology* 2 (4) (2008) 630–635.
- [18] M. Wilinska, L. Chassin, C. Acerini, J. Allen, D. Dunger, R. Hovorka, Simulation environment to evaluate closed-loop insulin delivery systems in type 1 diabetes, *Journal of Diabetes Science and Technology* 4 (1) (2010) 132–144.
- [19] G. Cocha, V. Constanza, C. D'Atellis, Control nolineal de la diabetes mellitus Tipo I, in: *Actas de la RPIC*, Rosario, Argentina, 2009, pp. 240–245.
- [20] R. Hovorka, V. Canonico, I. Chassin, U. Haueter, M. Massi-Benedetti, M.O. Federici, T. Pieber, H. Schaller, L. Schaupp, T. Vering, M. Wilinska, Nonlinear model predictive control of glucose concentration in subjects with type 1 diabetes, *Physiology Measurement* 25 (4) (2004) 905–920.
- [21] R. Sánchez Peña, A. Ghersin, LPV control of glucose for Diabetes type I, in: *Proceedings 32nd Annual International Conference, IEEE EMBS*, Buenos Aires, Argentina, 2010, pp. 680–683.
- [22] R. Sánchez Peña, A. Ghersin, F. Bianchi, Time varying procedures for diabetes type I control, *Journal of Electrical and Computer Engineering, special Issue Electrical and Computer Technology for Effective Diabetes Management and Treatment* 2011 (2011), Article ID 697543, 10 pages.
- [23] B. Kovatchev, M. Breton, C. Dalla-Man, C. Cobelli, In silico preclinical trials: a proof of concept in closed-loop control of type 1 diabetes, *Journal of Diabetes Science and Technology* 3 (1) (2009) 44–55.
- [24] M. Chamberlain, L. Stimmer, The renal handling of insulin, *Journal of Clinical Investigation* 46 (6) (1967) 911–919.
- [25] C. Dalla-Man, R. Rizza, C. Cobelli, Meal simulation model of the glucose–insulin system, *IEEE Transactions on Biomedical Engineering* 54 (10) (2007) 1740–1749.
- [26] C. Dalla-Man, D. Raimondo, R. Rizza, C. Cobelli, GIM, simulation software of meal glucose–insulin model, *Journal of Diabetes Science and Technology* 1 (3) (2007) 323–330.
- [27] C. Dalla-Man, C. Cobelli, A system model of oral glucose absorption: validation on gold standard data, *IEEE Transactions on Biomedical Engineering* 53 (12) (2006) 2472–2478.
- [28] R. Hovorka, F. Shojaee-Moradie, P. Carroll, L. Chassin, I. Gowrie, N. Jackson, R. Tudor, A. Umpleby, R. Jones, Partitioning glucose distribution/transport, disposal, and endogenous production during ivgtt, *American Journal of Physiology: Endocrinology Metabolism* 282 (2002) 992–1007.
- [29] B.H. Ginsberg, Factors affecting blood glucose monitoring: sources of errors in measurement, *Journal of Diabetes Science and Technology* 3 (4) (2009).
- [30] M. Safonov, D.J.N. Limebeer, R.V. Chiang, Simplifying the H_∞ theory via loop shifting, matrix pencil and descriptor concepts, *International Journal of Control* 50 (6) (1989) 2467–2488.
- [31] P. Gahinet, P. Apkarian, An LMI approach to H_∞ control, *International Journal of Robust and Nonlinear control* 4 (8) (1994) 421–448.